

Synthesis, structure and dynamics of *endo*- and *exo*-isomers of η^3 -allyl(η^5 -pentamethylcyclopentadienyl)dicarbonylrhenium tetrafluoroborate, $[(\eta^5\text{-C}_5\text{Me}_5)\text{Re}(\text{CO})_2(\eta^3\text{-C}_3\text{H}_5)][\text{BF}_4]$

Raymond J. Batchelor, Frederick W.B. Einstein ^{*}, Jun-Ming Zhuang and Derek Sutton ^{*}

Department of Chemistry, Simon Fraser University, Burnaby, B.C. V5A 1S6 (Canada)

(Received April 5th, 1990)

Abstract

The cationic η^3 -allyl complex $[\text{Cp}^*\text{Re}(\text{CO})_2(\eta^3\text{-C}_3\text{H}_5)][\text{BF}_4]$ (**1**) has been synthesized from the propene complex $\text{Cp}^*\text{Re}(\text{CO})_2(\eta^2\text{-C}_3\text{H}_6)$ (**2**) by reaction with $[\text{Ph}_3\text{C}][\text{BF}_4]$. The ^1H NMR spectrum of **1** in CD_2Cl_2 exhibits individual sets of methyl and allyl resonances corresponding to *endo* and *exo* isomers in an approximate ratio *endo*:*exo* = 6.4:1. The resonances that are identified with each isomer were determined by application of the nuclear Overhauser effect. Magnetization transfer results show that *endo*–*exo* interconversion occurs with no scrambling of *syn* and *anti* protons, consistent with a pseudorotation mechanism but not a η^3 – η^1 – η^3 mechanism. The crystal structure of **1** has been determined. The analysis gave a model in which both *endo* and *exo* isomers are present in an approximate ratio *endo*:*exo* = 4:6. Crystals of **1** are orthorhombic, space group *Pcab* with $a = 12.3142(12)$, $b = 12.8148(18)$, $c = 21.767(3)$ Å, $V = 3434.9$ Å³, $Z = 8$. The structure was refined to $R_F = 0.027$ and $R_{\text{w}F} = 0.038$ using 1480 observed intensities in the range $4 < 2\theta < 50^\circ$ ($l = 2n$); $4 < 2\theta < 40^\circ$ ($l = 2n + 1$) collected on an Enraf Nonius CAD-4F diffractometer with graphite monochromatized Mo- K_α radiation.

Introduction

The existence of isomers of $\text{CpMo}(\text{CO})_2(\eta^3\text{-C}_3\text{H}_5)$ was first noted by King [1] and was proposed by Davison and Rode [2] to result from different orientations of the allyl group (subsequently termed *endo* and *exo* [3]) on the basis of the temperature dependence of the allyl resonances in the NMR spectrum. Further work by Faller [4,5] allowed the individual sets of allyl resonances to be convincingly assigned to the appropriate *endo* or *exo* isomer, confirmed that there was no averaging of the *syn* and *anti* protons during the interconversion of the stereoisomers, and suggested that this interconversion occurs by pseudorotation of the allyl

Table 1
 ^1H NMR parameters for $[\text{Cp}^*\text{Re}(\text{CO})_2(\eta^3\text{-C}_3\text{H}_5)]\text{[BF}_4\text{]} (1)$ and related allyl complexes

Compound	Isomer	^1H NMR a (δ)				Solvent	Reference
		Cp/Cp*	H _c	H _s ^b	H _a ^c		
$[\text{Cp}^*\text{Re}(\text{CO})_2(\eta^3\text{-C}_3\text{H}_5)]\text{[BF}_4\text{]} (1)$	<i>endo</i>	2.17s	4.76m	3.83d[6.7]	1.77d[10.1]	CD_2Cl_2 ^d	This work
		2.21s	4.73m	3.82d[5.6]	1.87d[9.9]	CDCl_3 ^d	This work
$[\text{Cp}^*\text{Re}(\text{CO})_2(\eta^3\text{-C}_3\text{H}_5)]\text{[BF}_4\text{]} (1)$	<i>exo</i>	2.16s	3.83m	3.29d[7.0]	2.53d[10.9]	CD_2Cl_2 ^d	This work
		2.10s	4.06m	3.36d[6.7]	2.17d[10.8]	CDCl_3 ^d	This work
$[\text{CpRe}(\text{CO})_2(\eta^3\text{-C}_3\text{H}_5)]\text{[BF}_4\text{]}$	<i>endo</i>	6.352s	4.960tt	3.843d[6.1]	3.466d[10.4]	$(\text{CD}_3)_2\text{CO}$ ^e	8a
$[\text{CpRe}(\text{CO})_2(\eta^3\text{-C}_3\text{H}_5)]\text{[BF}_4\text{]}$	<i>exo</i>	6.379s	5.328tt	4.140d[7.0]	2.715d[10.7]	$(\text{CD}_3)_2\text{CO}$ ^e	8a
$[\text{CpMn}(\text{CO})_2(\eta^3\text{-C}_3\text{H}_5)]\text{[BF}_4\text{]}$	<i>endo</i>	5.886s	5.886tt	4.736d[6.9]	3.656d[11.2]	$(\text{CD}_3)_2\text{CO}$ ^e	8a
$[\text{CpMn}(\text{CO})_2(\eta^3\text{-C}_3\text{H}_5)]\text{[BF}_4\text{]}$	<i>exo</i>	5.840s	5.974tt	4.503d[7.0]	2.416d[11.4]	$(\text{CD}_3)_2\text{CO}$ ^e	8a
$\text{CpMo}(\text{CO})_2(\eta^3\text{-C}_3\text{H}_5)$	<i>endo</i>	5.10s	3.58m	2.72d[6.4]	1.76d[10.5]	CDCl_3 ^g	5a
$\text{CpMo}(\text{CO})_2(\eta^3\text{-C}_3\text{H}_5)$	<i>exo</i>	5.10s	3.92m	2.78d[7.3]	0.88d[10.8]	CDCl_3 ^g	5a
$\text{CpW}(\text{CO})_2(\eta^3\text{-C}_3\text{H}_5)$	<i>endo</i>	5.22s	3.67m	2.70d[5.6]	1.64d[9.5]	CDCl_3 ^g	5a
$\text{CpW}(\text{CO})_2(\eta^3\text{-C}_3\text{H}_5)$	<i>exo</i>	5.25s	3.54m	2.73d[6.9]	1.07d[10.4]	CDCl_3 ^g	5a
$\text{CpRu}(\text{CO})_2(\eta^3\text{-C}_3\text{H}_5)$	<i>endo</i>	5.17s	4.08m	3.03d[6.3]	1.80d[11.0]	CDCl_3 ^f	7a
$\text{CpRu}(\text{CO})_2(\eta^3\text{-C}_3\text{H}_5)$	<i>exo</i>	5.04s	4.07m	2.92d[6.9]	1.28d[10.6]	CDCl_3 ^f	7a

^a Chemical shifts are given in ppm downfield from TMS; H_c, H_s and H_a are the central, *syn* and *anti* protons of C_3H_5 ; s, singlet; d, doublet; t, triplet; m, multiplet. All coupling constants are absolute values. ^b $J(\text{H}_c\text{H}_s)$ in brackets. ^c $J(\text{H}_c\text{H}_a)$ in brackets. ^d Recorded at 400 MHz. ^e Recorded at 200 MHz. ^f Recorded at 90 MHz. ^g Recorded at 100 MHz.

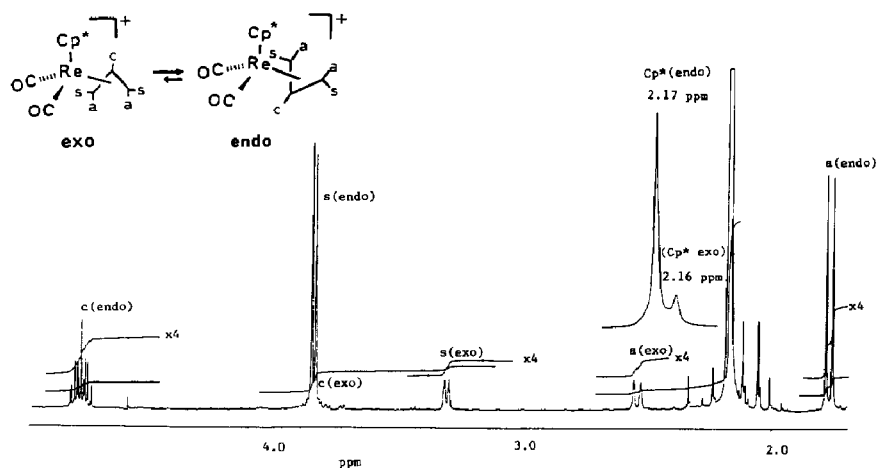


Fig. 1. 400 MHz ^1H NMR spectrum of **1** in CD_2Cl_2 at room temperature showing individual resonances for *endo* and *exo* isomers (*endo/exo* = 6:4).

(Similarly, the IR ($\nu(\text{CO})$) spectra of the Cp analogue, $[\text{CpRe}(\text{CO})_2(\eta^3\text{-allyl})][\text{BF}_4]$, was reported [8a] to display two sets of bands at 2060, 2004 cm^{-1} (*endo*); 2047, 1982 cm^{-1} (*exo*) in CH_3NO_2). The complex was further characterized by the positive ion fast atom bombardment spectrum which displayed the molecular mass of the cation at m/z 419 with the appropriate ^{187}Re , ^{185}Re isotope pattern, together with peaks corresponding to the loss of CO and, interestingly, C_3H_6 . Finally, the X-ray crystal structure was determined as described below.

^1H NMR spectral assignments for $[\text{Cp}^*\text{Re}(\text{CO})_2(\eta^3\text{-C}_3\text{H}_5)][\text{BF}_4]$ (**1**)

The room temperature 400 MHz ^1H NMR spectrum of **1** in CD_2Cl_2 exhibits methyl and AMM'XX' allyl resonances for two isomers in approximate ratio 6.4:1 (Fig. 1 and Table 1). For the major isomer the multiplet at δ 4.76 is assigned to H_c , and the doublets at δ 3.83 and δ 1.77 are assigned to the *syn* and *anti* protons H_s and H_a respectively. This assignment is in accord with ample precedent for allyl ligands in symmetrical environments, and with the greater separation of the doublet in H_a arising from the larger coupling constant H_cH_a compared with H_cH_s [12,13]. For the minor isomer the resonances for H_a and H_s are clearly visible, but the H_c resonance is buried under the H_s signal of the major isomer. This is established by decoupling experiments and also by integration and the results of saturation transfer experiments. In addition, the ^1H NMR spectrum of **1** in CDCl_3 clearly shows the multiplet for H_c of the minor isomer at δ 4.06, quite well separated from the H_s resonance of the major isomer at δ 3.82 in this solvent.

The major isomer is assigned as the *endo* isomer from the results of nuclear Overhauser enhancement (NOE) studies. Saturation of the Cp^* methyl resonances results in a strong NOE at the δ 1.77 (H_a) signal for the major isomer (Fig. 2). In the absence of exchange this would unquestionably establish that this resonance arises from the *endo* isomer since in the *exo* isomer the *anti* protons are remote from the Cp^* methyls. However, exchange between *endo* and *exo* isomers is indeed occurring as is evident, for example, from Fig. 3, where saturation of this resonance results in transfer of magnetization to the signal at δ 2.53, assigned as H_a of the minor isomer. But this does not invalidate the result.

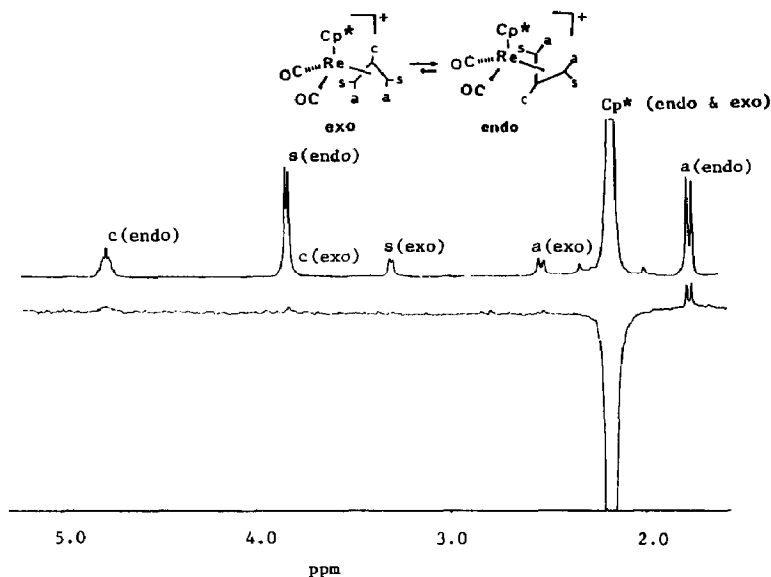


Fig. 2. NOE difference spectrum (lower trace) for **1** obtained upon saturating the methyl resonances of the pentamethylcyclopentadienyl group in the *endo* and *exo* isomers. Note the strong NOE enhancement of the *endo* H_a signal and weaker enhancement of *endo* H_c and *exo* H_c signals.

Let us, for the moment, consider the other alternative, that the signal at δ 1.77 is the *anti* resonance of a major *exo* isomer. Enhancement of this resonance cannot arise directly by an NOE from the *exo* isomer's methyls. Could it arise from exchange with the *anti* protons of a minor *endo* isomer, which clearly would experience an NOE from the *endo* isomer's methyls? If that were so an enhance-

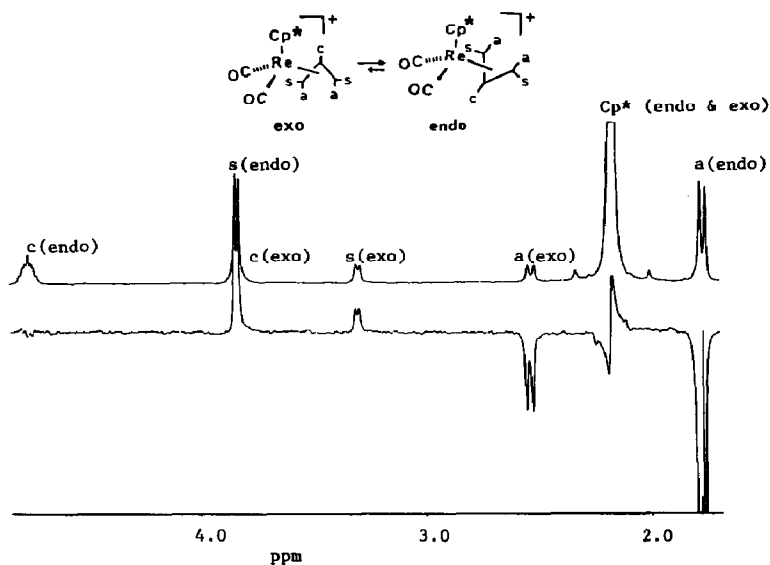


Fig. 3. NOE difference spectrum for **1** obtained upon saturating the *endo* H_a resonance. Note transfer of saturation to the H_a resonance of the *exo* isomer only, and NOE enhancement of the *syn* proton signals H_s of the *endo* and *exo* isomers.

ment of the *endo* isomer's *anti* protons at δ 2.53 should also be observed and should be relatively as large or larger than the enhancement at δ 1.77 to allow for NOE buildup at this latter position [14]. No detectable enhancement is observed at δ 2.53 position in Fig. 2, even though the rate of exchange is clearly significant as judged from the observed saturation transfer in Fig. 3. On this basis we rule out the second possibility.

Irradiation of the Cp* methyls should also give a NOE to H_c in the minor *exo* isomer; in agreement a weak but detectable enhancement is observed together with a similarly weak enhancement of H_c (*endo*) because of exchange. The results of irradiating H_a (*endo*), Fig. 3, demonstrate that no *syn-anti* exchange occurs. There is the expected strong NOE to the *endo syn* protons H_s and a corresponding enhancement of H_s (*exo*) is also observed because of exchange. However, no transfer of saturation from H_a (*endo*) to H_s (*endo* or *exo*) signals occurs. Comparable results were obtained on irradiating H_s (*endo* or *exo*), or H_a (*exo*). Irradiation at H_s (*endo*) necessarily implies also saturation of H_c (*exo*) if, as is proposed, these are coincident; in agreement, a strong inverted signal at H_c (*endo*) resulted because saturation is transferred from H_c (*exo*) to H_c (*endo*), so confirming the assignment of H_c (*exo*) to this position.

The saturation transfer results indicate that the interconversion of the *endo* and *exo* isomers in **1** proceeds by pseudorotation of the allyl group since this mechanism does not scramble the *syn* and *anti* protons. Similar *endo* and *exo* isomers that also appear to interconvert by this mechanism are CpM(CO)₂(η^3 -C₃H₅) (M = Mo, W) [5] and the cations [CpM(CO)₂(η^3 -allyl)]⁺ (M = Mn, Re) [8]. For the neutral Mo and W complexes the predominant isomer in the mixture is the *exo* form, which becomes destabilized in the methylallyl analogue [4]. Evidently the *exo* isomer also predominates in the cationic Mn complex, though the reports of this compound differ in the ability to observe individual resonances for the isomers [8]. However, the cationic rhenium complex was observed to be predominantly the *endo* isomer [8a] and we arrive at the same conclusion for the pentamethylcyclopentadienyl analogue (**1**) here.

One final point about the NMR spectrum of **1** should be made, which is in regard to the relative positions of the resonances for the *endo* and *exo* isomers. These are listed in Table 1 along with literature values for related compounds. Hitherto, for cyclopentadienyl complexes, an empirical generalization has been that the H_a protons of the *exo* isomer resonate most upfield [5a]. This is not the case for the pentamethylcyclopentadienyl complex (**1**), where H_a of the *endo* isomer is the most upfield resonance. Unfortunately, the only other isomeric pentamethylcyclopentadienyl allyl complex to have been studied, Cp*W(CO)₂(η^3 -C₃H₅), evidently only gave an averaged spectrum in the temperature range examined [9a]. The pentamethylcyclopentadienyl complex (η^5 -C₅Me₅)RuCl₂(η^3 -C₃H₅) has also recently been reported. The *endo* isomer was present in the solid state and in solution; no isomerization to *exo* was observed [9b].

*X-Ray structure of [Cp*Re(CO)₂(η^3 -C₃H₅)] [BF₄] (**1**)*

The structure of the cation of **1** is illustrated in Fig. 4. The most evident feature is the disorder of the allyl group, that is to say the crystals are composed of both *endo* and *exo* isomers. The final occupancies of the two sites give the approximate distribution of the isomers to be 4:6 *endo:exo*. In most of the other cases where

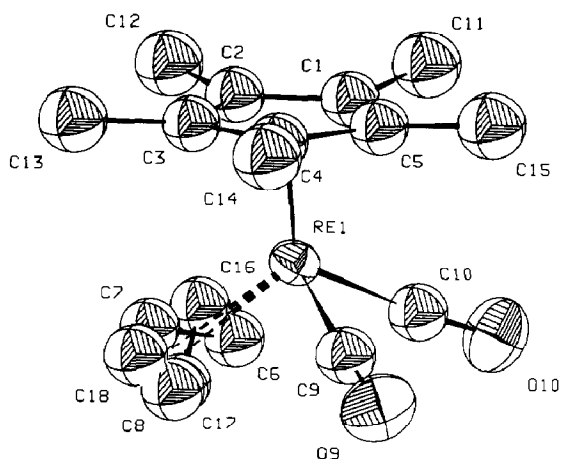


Fig. 4. View of the cationic η^3 -allyl complex in $[\text{Cp}^*\text{Re}(\text{CO})_2(\eta^3\text{-C}_3\text{H}_5)][\text{BF}_4]$ **1** with atom numbering. Note the disorder of the allyl group (superposition of *endo* and *exo* isomers in ratio *endo:exo* 4:6). Hydrogen atoms have been omitted for clarity.

endo and *exo* isomers have been evident in solution, only one of the isomers crystallizes and the equilibrium readjusts the concentrations of the two isomers as crystallization proceeds. For example, $\text{CpMo}(\text{CO})_2(\eta^3\text{-C}_3\text{H}_5)$ [15] and

Table 2

Selected bond distances (\AA) and angles ($^\circ$) for $[\text{Cp}^*\text{Re}(\text{CO})_2(\eta^3\text{-C}_3\text{H}_5)][\text{BF}_4]$ (**1**)

<i>Distances</i>			
Re(1)–C(9)	1.92(1)	Re(1)–C(10)	1.93(1)
Re(1)–C(1)	2.26(1)	Re(1)–C(2)	2.34(1)
Re(1)–C(3)	2.32(1)	Re(1)–C(4)	2.26(1)
Re(1)–C(5)	2.23(1)	Re(1)–C(6)	2.29(3)
Re(1)–C(7)	2.23(2)	Re(1)–C(8)	2.24(3)
Re(1)–C(16)	2.26(4)	Re(1)–C(17)	2.33(4)
Re(1)–C(18)	2.33(4)	Re(1)–Cp* ^a	1.93
O(10)–C(10)	1.14(2)	O(9)–C(9)	1.16(1)
C(7)–C(8)	1.45(4)	C(6)–C(7)	1.42(4)
C(17)–C(18)	1.47(6)	C(16)–C(17)	1.33(6)
<i>Angles</i>			
C(10)–Re(1)–C(9)	84.9(5)	C(16)–Re(1)–C(9)	126.5(11)
C(6)–Re(1)–C(9)	115.9(10)	C(17)–Re(1)–C(9)	95.0(12)
C(7)–Re(1)–C(9)	110.3(8)	C(18)–Re(1)–C(9)	81.9(12)
C(8)–Re(1)–C(9)	73.1(8)	C(16)–Re(1)–C(10)	84.2(11)
C(6)–Re(1)–C(10)	70.9(9)	C(17)–Re(1)–C(10)	91.9(13)
C(7)–Re(1)–C(10)	106.2(7)	C(18)–Re(1)–C(10)	124.5(12)
C(8)–Re(1)–C(10)	109.7(10)	Cp*–Re(1)–C(16)	114
Cp*–Re(1)–C(6)	127	Cp*–Re(1)–C(17)	136
Cp*–Re(1)–C(7)	116	Cp*–Re(1)–C(18)	115
Cp*–Re(1)–C(8)	131	Cp*–Re(1)–C(10)	119
Cp*–Re(1)–C(9)	117	O(10)–C(10)–Re(1)	174.0(13)
O(9)–C(9)–Re(1)	176.5(13)	C(18)–C(17)–C(16)	117(5)
C(8)–C(7)–C(6)	110(4)		

^a Cp* = the centre of mass of the C₅ ring.

$\text{Cp}^*\text{W}(\text{CO})_2(\eta^3\text{-C}_3\text{H}_5)$ [9a] have both been structurally analyzed as the *exo* isomers. In only very rare cases is it possible to isolate, crystallize and determine the structure of both the *endo* and *exo* isomers of an allyl complex. Where the interconversion is either sufficiently slow or non-existent, isomers may be separated by chromatography or fractional crystallization [7,10]. This has been achieved with $\text{Cp}^*\text{Re}(\text{CO})(\text{H})(\eta^3\text{-C}_3\text{H}_5)$ [10] and the 2-methylallyl complex $\text{CpRu}(\text{CO})(\eta^3\text{-C}_4\text{H}_7)$ [16a]. Alternatively, different synthetic strategies may be employed for synthesis of the *exo* and *endo* forms, as was the case in the recent structure determination of the *exo* and *endo* phenylallyl complexes $[\text{CpMo}(\text{CO})(\text{NO})(\eta^3\text{-C}_3\text{H}_4\text{Ph})][\text{BF}_4]$ [16b]. Despite numerous other structure determinations of *endo* and *exo* allyl isomers (many of these are cited in references 10 and 16) we know of no previous case where both isomers have occurred in a disordered structure. Unfortunately, the presence of the disorder means that the allyl carbon positions are not determined with sufficient precision to warrant a detailed discussion of the metrical details (Table 2), either by comparing the isomers with one another or with previous structures, save that the distances and angles are chemically reasonable, albeit with large errors.

Experimental

Synthetic work was carried out by using standard Schlenk techniques under dry nitrogen. Solvents were dried by standard methods and were distilled and stored under nitrogen. IR spectra were run on a Perkin-Elmer 983G instrument in CaF_2 cells. ^1H NMR spectra and the NOE runs were obtained by Mrs. M.M. Tracey on a Bruker WM-400 instrument at 400 MHz. FAB-MS spectra were obtained by Mr. G. Owen on a Hewlett-Packard 5985 GCMS instrument fitted with a Phrasor Scientific Inc. FAB accessory, using Xe bombardment and samples dispersed in a thioglycerol matrix. Elemental analyses were performed by Mr. M.K. Yang of the SFU Micro-analytical Laboratory.

Synthesis of $[\text{Cp}^\text{Re}(\text{CO})_2(\eta^3\text{-C}_3\text{H}_5)][\text{BF}_4]$ (1)*

A solution of $[\text{Ph}_3\text{C}][\text{BF}_4]$ (80 mg; 0.24 mmol) in nitromethane (0.5 mL) was added to a solution of $\text{Cp}^*\text{Re}(\text{CO})_2(\eta^2\text{-C}_3\text{H}_6)$ [10] (81 mg; 0.19 mmol) in nitromethane (1 mL) and the solution was heated at 60°C for 5 minutes. The IR spectrum indicated that reaction was complete. The mixture was poured into dry Et_2O (100mL) and stirred for 20 minutes to ensure removal of trityl fluoroborate, then filtered. The colourless product obtained was recrystallized from CH_2Cl_2 -hexane. Analysis. Found: C, 35.45; H, 4.01. Calcd for $\text{C}_{15}\text{H}_{20}\text{BF}_4\text{O}_2\text{Re}$: C, 35.65; H, 3.99. IR (CH_2Cl_2 , cm^{-1}) 2053s, 1999s, ($\nu(\text{CO})$), IR(MeNO_2 , cm^{-1}) 2060s, 2004s, (*endo*); 2047s, 1982s (*exo*) ($\nu(\text{CO})$), FAB-MS (thioglycerol, ^{187}Re) m/z 419(M^+ of cation), 391($M^+ - \text{CO}$), 377($M^+ - \text{C}_3\text{H}_6$), 349($M^+ - \text{C}_3\text{H}_6 - \text{CO}$). ^1H NMR, see Table 1.

X-Ray crystal structure determination for 1

A suitable crystal of **1**, grown from a solution in CH_2Cl_2 -hexane, was mounted on a glass fiber with epoxy resin. Intensity data were collected with an Enraf Nonius CAD-4F diffractometer using graphite monochromatized Mo-K_α radiation. The unit cell was determined from 25 well-centered reflections in the range $18 < 2\theta < 21^\circ$. Two intensity standards were measured every 80 min. of acquisition time, and these showed no significant variations in intensity during the data acquisition. The data

were corrected analytically for absorption [17] (transmission range 0.216–0.314) and data reduction included intensity scaling and Lorentz and polarization corrections.

1 displays a subcell of a , b , $c/2$. The average intensity of the $l = 2n + 1$ data is $\approx 10^{-2}$ that of the $l = 2n$ data. Initial structure solution using only the half-cell, in $Pmab$, produced a disordered structural model ($R = 0.042$, $N_{\text{obs}} = 1174$, $N_{\text{var}} = 92$) whose asymmetric unit consisted of one complete “molecule”, at half occupancy, with the Re atom on the crystallographic mirror plane. A Patterson map derived from only the $l = 2n + 1$ data indicated small displacements of the Re atoms from the mirror plane. The space group $Pcab$ for the “full cell” was determined by refinement of the positions of 8 Re atoms in $P1$ subject to “Waser”-type restraints * limiting the coordinate shifts. Subsequent Fourier syntheses yielded an ordered model for the cation with two site disorder for the atoms of the BF_4^- anion, ($R = 0.030$, $N_{\text{obs}} = 1480$, $N_{\text{var}} = 106$). The C–C bond distances and C–C–C bond angle of the allyl group and the magnitudes of the isotropic temperature factors for these carbon atoms suggested unresolved disorder for this group. A model including two fractionally occupied sites for each of the allyl carbon atoms was refined with a

Table 3

Crystallographic data for the structure determination of $[\text{Cp}^*\text{Re}(\text{CO})_2(\eta^3\text{-C}_3\text{H}_5)]\text{[BF}_4\text{]} (1)$

Formula	$\text{C}_{15}\text{H}_{20}\text{BF}_4\text{O}_2\text{Re}$
Crystal system	orthorhombic
Space group	$Pcab$ (No. 61)
a (Å)	12.314(2)
b (Å)	12.815(2)
c (Å)	21.767(3)
V (Å ³)	3434.9
Z	8
FW	505.33
ρ_c (g cm ⁻³)	1.954
μ (Mo- K_α) (cm ⁻¹)	72.13
Crystal size (mm)	0.2 × 0.3 × 0.4
λ (Å)	0.71069
Transmission	0.216–0.314
Scan mode	$\omega - 2\theta$
Scan width ^a (°)	1.0 + 0.35 tan θ
Scan speed (° min ⁻¹)	0.8–3.3 ($l = 2n$) ^b ; 1.1 ($l = 2n + 1$)
Min-max 2θ (°)	4–50 ($l = 2n$); 4–40 ($l = 2n + 1$)
Unique data	1586 ($l = 2n$); 842 ($l = 2n + 1$)
Obsvd data ^c	1174 ($l = 2n$); 306 ($l = 2n + 1$)
Restraints	20
Rfnd params	125
$R(F)$ ^d	0.027
$R_w(F)$ ^e	0.038
G.O.F. ^f	1.00
Max pk (e Å ⁻³)	0.9(3) ^g
Max shift/error	0.01

^a The background intensities were estimated by extension of the predetermined scan angle by 25% on either side. ^b The final scan speed was determined from the intensity of a preliminary scan. ^c $I_o \geq 2.5\sigma(I_o)$. ^d $R(F) = \Sigma(|F_o| - |F_c|) / \Sigma|F_o|$; for observed data. ^e $R_w(F) = [\Sigma(w(|F_o| - |F_c|)^2) / \Sigma(wF_o^2)]^{1/2}$; for observed data, where: $w = [54.3563 t_0(x) + 52.6887 t_1(x)]^{-1}$, $x = |F_o| / F_{\text{max}}$ and t_n are the polynomial functions of the Chebyshev series; J.R. Carruthers and D.J. Watkin, Acta Crystallogr., A35 (1979) 698. ^f G.O.F. = $[\Sigma w(|F_o| - |F_c|)^2 / \text{degrees of freedom}]^{1/2}$. ^g 0.98 Å from Re.

Table 4

Coordinates ($\times 10^4$) and isotropic or equivalent isotropic temperature factors ($\text{\AA}^2 \times 10^4$) for the non-hydrogen atoms of $[\text{Cp}^*\text{Re}(\text{CO})_2(\eta^3\text{-C}_3\text{H}_5)][\text{BF}_4]$ (1)

Atom	x	y	z	U_{iso}
Re(1)	2416(1)	5146.8(3)	788.5(2)	393
O(9)	4211(8)	6684(8)	410(6)	697
O(10)	1001(9)	6297(9)	-155(5)	793
C(9)	3538(11)	6091(10)	535(7)	568(23)
C(10)	1545(11)	5834(10)	170(7)	568(23)
C(6) ^a	1879(25)	3946(23)	73(17)	579(65)
C(7) ^a	2750(19)	3551(18)	432(12)	568(58)
C(8) ^a	3707(23)	4186(21)	335(15)	649(56)
C(16) ^b	1901(36)	3670(31)	301(18)	579(65)
C(17) ^b	2909(33)	3829(33)	108(25)	568(58)
C(18) ^b	3761(33)	3917(33)	580(20)	649(56)
C(1)	1050(10)	5433(10)	1462(6)	538(13)
C(2)	1431(11)	4412(10)	1602(6)	543(13)
C(3)	2569(17)	4516(8)	1785(4)	543(13)
C(4)	2836(9)	5583(10)	1765(5)	543(13)
C(5)	1897(11)	6164(10)	1565(6)	545(13)
C(11)	-93(12)	5697(12)	1325(7)	750(19)
C(12)	810(13)	3416(12)	1603(7)	750(19)
C(13)	3268(12)	3642(11)	2030(7)	750(19)
C(14)	3882(12)	6025(12)	2008(7)	750(19)
C(15)	1791(13)	7338(12)	1553(7)	750(19)
F(1) ^c	2359(24)	4734(17)	3312(10)	1359(31)
F(2) ^c	2374(24)	6233(16)	3808(11)	1359(31)
F(3) ^c	1001(20)	5148(19)	3886(12)	1359(31)
F(4) ^c	1272(21)	5999(20)	3023(11)	1359(31)
F(11) ^c	1385(20)	6040(19)	4052(10)	1359(31)
F(12) ^c	2652(21)	6203(17)	3361(10)	1359(31)
F(13) ^c	2225(20)	4674(16)	3717(11)	1359(31)
F(14) ^c	1095(21)	5597(19)	3101(12)	1359(31)
B(1) ^c	1753(15)	5514(12)	3504(7)	374(29)
B(11) ^c	1839(15)	5617(13)	3555(7)	374(29)

^a Occupancy = 0.60(3). ^b Occupancy = 0.40. ^c Occupancy = 0.50(2). General equivalent positions: x, y, z ; $-x, 1/2 - y, 1/2 + z$; $1/2 - x, 1/2 + y, -z$; $1/2 + x, -y, 1/2 - z$; $-x, -y, -z$; $x, 1/2 + y, 1/2 - z$; $1/2 + x, 1/2 - y, z$; $1/2 - x, y, 1/2 + z$.

single isotropic temperature factor for the allyl ensemble. The refined positions of the six carbon sites were consistent with two reasonable orientations of the π -allyl group representing *endo*- and *exo*-isomers of the complex. The hydrogen atoms were placed in calculated positions and during further refinement were allowed to ride on their respective carbon atoms. The final cycles of refinement included a single isotropic temperature factor for each of the following sets of atoms: C(9), C(10); C(6), C(16); C(7), C(17); C(8), C(18); C(11)–C(15); all fluorine atoms; B(1), B(11); all allyl hydrogen atoms; all methyl hydrogen atoms. Anisotropic thermal parameters were refined for rhenium and oxygen atoms. The Cp^{*}-ring carbon atoms were

* These are soft restraints included as 'observations' in the L.S. summations, after: (a) J. Waser, *Acta Cryst.*, 16, (1963) 1091; (b) J.S. Rollett in *Crystallographic Computing*, Munksgaard, Copenhagen (1970) 170.

each allowed independent isotropic temperatures factor. All cycles of refinement included an independent scale factor for the $l = 2n + 1$ data as these had been acquired differently and were scaled independently by the data reduction program. The maximum $|\text{shift}/\text{esd}|$ was ≤ 0.01 for the final full matrix least-squares refinement of 125 parameters for 1480 observations ($I_o \geq 2.5\sigma(I_o)$) and 20 restraints. The largest peak in the final difference map ($0.9(3) \text{ e}\text{\AA}^{-3}$) occurred 0.98 \AA from Re.

A weighting scheme was applied such that $\langle w(|F_o| - |F_c|)^2 \rangle$ was near constant as a function of both $|F_o|$ and $\sin \theta/\lambda$. Complex scattering factors for neutral atoms were used in the calculation of structure factors [18]. The programs used for data reduction, structure solution and refinement were from the NRC VAX Crystal Structure System [19]. The program CRYSTALS [20] was employed in the final refinement involving the use of restraints. The diagram (Fig. 4) was generated with the program SNOOPI [21]. All computations were carried out on a MICRO VAX-II computer.

Crystallographic data are summarized in Table 3. The final positional and isotropic or equivalent isotropic thermal parameters for the non-hydrogen atoms are given in Table 4. Coordinates and temperature factors for the hydrogen atoms, anisotropic temperature factors for rhenium and oxygen atoms and a table of observed and calculated structure factors are available from the authors.

Acknowledgements

We thank Dr. A.S. Tracey for assistance with the NOE experiments and for helpful discussions. This work was supported by an operating grant from NSERC Canada.

References

- 1 R.B. King, *Inorg. Chem.*, 5 (1966) 2242.
- 2 A. Davison and W.C. Rode, *Inorg. Chem.*, 6 (1967) 2124.
- 3 J.W. Faller and A.M. Rosan, *J. Am. Chem. Soc.*, 98 (1976) 3388.
- 4 J.W. Faller and M.J. Incorvia, *Inorg. Chem.*, 7 (1968) 840.
- 5 (a) J.W. Faller, C.-C. Chen, M.J. Mattina and A. Jakubowski, *J. Organomet. Chem.*, 52 (1973) 361; (b) J.W. Faller and A. Jakubowski, *ibid.*, 31 (1971) C75.
- 6 R.W. Fish, W.P. Giering, D. Marten and M. Rosenblum, *J. Organomet. Chem.*, 105 (1976) 101.
- 7 (a) D.H. Gibson, W.-L. Hsu, A.L. Steinmetz and B.V. Johnson, *J. Organomet. Chem.*, 208 (1981) 89. (b) D.H. Gibson and W.-L. Hsu, *Organomet. Synth.*, 4 (1988) 227. (c) J.W. Faller, B.V. Johnson and T.P. Dryja, *J. Organomet. Chem.*, 65 (1974) 395.
- 8 (a) V.V. Krivykh, O.V. Gusev, P.V. Petrovskii and M.I. Rybinskaya, *J. Organomet. Chem.*, 366 (1989) 129. (b) A.M. Rosan, *J. Chem. Soc., Chem. Commun.*, (1981) 311. (c) B. Buchmann and A. Salzer, *J. Organomet. Chem.*, 295 (1985) 63. (d) A.M. Rosan and D.M. Romano, *Organometallics*, 9 (1990) 1048.
- 9 (a) H.G. Alt, H.E. Engelhardt, B. Wrackmeyer and R.D. Rogers, *J. Organomet. Chem.*, 379 (1989) 289. (b) H. Nagashima, K. Mukai, Y. Shiota, K. Yamaguchi, K. Ara, T. Fukahori, H. Suzuki, M. Akita, Y. Moko-oka and K. Itoh, *Organometallics*, 9 (1990) 799.
- 10 R.J. Batchelor, F.W.B. Einstein, R.H. Jones, J.-M. Zhuang and D. Sutton, *J. Am. Chem. Soc.*, 111 (1989) 3468.
- 11 V.V. Krivykh, O.V. Gusev and M.I. Rybinskaya, *J. Organomet. Chem.*, 362 (1989) 351.
- 12 M.L.H. Green and P.L.I. Nagy, *Adv. Organomet. Chem.*, 2 (1964) 325.
- 13 A. Yamamoto, *Organotransition Metal Chemistry*, Wiley-Interscience, New York, 1986, p. 183.

- 14 J.K. Saunders and R.A. Bell, *Can. J. Chem.*, 48 (1970) 512.
- 15 J.W. Faller, D.F. Chodosh and D. Katahira, *J. Organomet. Chem.*, 187 (1980) 227.
- 16 (a). L.-Y. Hsu, C.E. Nordman, D.H. Gibson and W.-L. Hsu, *Organometallics*, 8 (1989) 241. (b) J.W. Faller, C. Lambert and M.R. Mazzieri, *J. Organomet. Chem.*, 383 (1990) 161.
- 17 J. DeMeulenaer and H. Tompa, *Acta Crystallogr.*, 19 (1965) 1014.
- 18 *International Tables for X-ray Crystallography*, Kynoch Press, Birmingham, England, 1975, Vol IV, p. 99.
- 19 E.J. Gabe, A.C. Larson, F.L. Lee and Y. LePage, NRC VAX Crystal Structure System, National Research Council, Ottawa, Canada, 1984.
- 20 D.J. Watkin, J.R. Carruthers and P.W. Betteridge, *CRYSTALS*, Chemical Crystallography Laboratory, University of Oxford, Oxford, England, 1985.
- 21 E.K. Davies, SNOOPI Plot Program, Chemical Crystallography Laboratory, University of Oxford, Oxford, England, 1985.